ELSEVIER

Chemical Engineering Journal 132 (2007) 9–15

Chemical Engineering Journal

www.elsevier.com/locate/cej

Characteristics of gas–solid mass transfer in a cocurrent downflow circulating fluidized bed reactor

Baolin Luo [a], Dong Yan [a], Ying L. Ma [b], Shahzad Barghi [b], Jesse Zhu [b,*]

[a] *Institute of Process Engineering, Chinese Academy of Sciences, Beijing 100080, China*

[b] *Department of Chemical and Biochemical Engineering, University of Western Ontario, London, Ontario, Canada N6A 5B9*

Received 19 September 2006; received in revised form 22 December 2006; accepted 2 January 2007

Abstract

The characteristics of gas–solids mass transfer were studied in a downer reactor with the adsorption of CO_2 tracer by activated charcoal particle. Axial distribution profiles of the CO_2 tracer concentration were measured under several different operating conditions. Mass transfer coefficient and axial dispersion coefficient were evaluated with a non-linear regressing method (Marquardt method). It was found that the operating conditions such as solids circulation rate and gas velocity have complicated effects on the gas–solids mass transfer coefficient, and the effect of superficial gas velocity seemed to be more significant than that of solids circulation rate.

The following empirical correlations were found to best fit the experimental data for axial dispersion coefficient, E_a and overall mass transfer coefficient, K_F:

$$Pe_1 = \frac{Lu_g}{E_a} = 0.226 Re^{0.499} m^{0.302}$$

$$Pe_2 = \frac{u_g}{K_F a L} = 0.000185 Re^{0.618} m^{-0.983}$$

with $m = G_s/(u_g \rho_p) = v_s(1-\varepsilon)/(u_g \varepsilon)$.

Keywords: Downflow circulating fluidized bed; Gas–solids mass transfer; Steady-state adsorption

1. Introduction

The cocurrent downflow circulating fluidized bed (downer) is a new type of fluidized bed reactor with great potential in commercial applications. In petrochemical industry, the downer has been regarded as a possible future and better alternative to the upflow fluidized bed (riser) for certain reactions since it is a quick contact reaction system and has such significant advantages as more uniform gas and solids flow structure, reduced axial dispersion and uniform gas and solids residence times [1–3]. Therefore in the last decade, the hydrodynamics in the new downer system have been studied by several research groups and considerable attention has been paid to its development [4–10].

However, most of the previous research in the downer was limited to its hydrodynamic characteristics such as two-phase flow behaviour, profiles of pressure gradient, solids concentration and velocity distributions. Wei et al. [4] studied gas dispersion in a downer with a steady-state tracer experiment. Zhu et al. [11] studied the radial gas–solids mixing in the entrance region through heat transfer measurements. Richardson and Backhtier [12] and Szckely [13] have reported the use of adsorption methods to study the gas–solids mass transfer in fluidized beds. They found that the rate of physical adsorption is much faster than that of diffusion so that adsorption cannot be the controlling step in the whole mass transfer process. Thus, it is feasible to study mass transfer in a fluidized bed using the adsorption method. In some of the previous studies, solids were weighed to quantify the adsorption [14,15]. This needs precision instrument, complex operation and still often leads to poor

* Corresponding author at: Department of Chemical and Biochemical Engineering, Faculty of Engineering, The University of Western Ontario, London, Ontario, Canada N6A 5B9. Tel.: +1 519 661 3807; fax: +1 519 661 3498.

E-mail address: jzhu@uwo.ca (J. Zhu).

1385-8947/$ – see front matter © 2007 Elsevier B.V. All rights reserved.
doi:10.1016/j.cej.2007.01.008

Nomenclature

a	specific surface area of adsorbent (1/m)
c	molar concentration of adsorbate in gas bulk (mol/m^3)
c_0	initial molar concentration of the tracer gas at the reactor entrance (mol/m^3)
c_i	interfacial molar concentration of the tracer gas (mol/m^3)
c^*	molar concentration of the tracer gas in equilibrium with q_i (mol/m^3)
C	dimensionless concentration, c_i/c_0
dt	time required for the solids to pass through the differential section of the downer (s)
dx	the height of the differential section of the downer (m)
D_e	efficient diffusion coefficient in the inner cavity (m^2/s)
E_a	axial dispersion coefficient in gas phase (m^2/s)
F_a	mass flow rate of gas phase (kg/s)
G_s	solids circulation rate (kg/m^2 s)
k_f	mass transfer coefficient in the gas film (m/s)
k_s	mass transfer coefficient in the film of solids side (m/s)
K_F	overall mass transfer coefficient defined with difference of concentration (m/s)
K_s	overall mass transfer coefficient defined with difference of adsorbed quantity (kg/m^2 s)
L	total height of downer (m)
m	volumetric solids to gas ratio ($=G_s/(u_g\rho_p) = v_s(1-\varepsilon)/u_g$)
Pe_1	Peclet Number of axial dispersion
Pe_2	Peclet Number of mass transfer
q	adsorbed tracer gas quantity per unit weight of particles (mol/kg)
q_i	adsorbed tracer gas quantity in equilibrium with interface concentration (mol/kg)
q^*	adsorbed tracer gas quantity in equilibrium with gas concentration (mol/kg)
R	particle radius (m)
Re_p	particle Reynolds number
s	cross-sectional area of the downer (m^2)
t	time (s)
u_g	superficial gas velocity (m/s)
v_s	actual particle velocity (m/s)
x	axial distance from the downer top (m)
y	molar fraction of the absorbate in gas bulk
Z	dimensionless distance from the downer top ($=x/L$)

Greek letters

β	Henry's coefficient (m^3/kg)
γ	overall mass transfer rate (mol/m^3 s)
γ_a	mass transfer rate of adsorption in gas interface film (mol/m^3 s)
γ_b	mass transfer rate in the film of solids phase (mol/m^3 s)
ε	bed voidage
Φ	dimensionless number for adsorption equilibrium
ρ_b	bed density (kg/m^3)
ρ_p	particle density (kg/m^3)

accuracy in the measurements. Another measurement method is the dynamic method [16], which requires rapid and continuous measurement of the adsorbate concentration in the inlet/outlet gas streams and a sophisticated method for data analysis.

So far, the gas–solids mass transfer behaviour in the downer has still not been directly measured. Since the gas–solids mass transfer rate is an extremely important parameter to control the reaction rate and selectivity, to obtain uniform product distribution, to maximize the yield for desirable intermediate products, and to avoid over-reaction, further studies of the characteristics of gas–solids mass transfer is essential for the design and development of downer reactors. In the downer, because the solid particles are renewed constantly, the adsorption process is different from that in fixed beds and other non-circulating fluidized beds, so that it is more difficult to set up an appropriate model to obtain the mass transfer data by the dynamic adsorption method. Therefore, a method with the steady-state adsorption of CO_2 gas tracer by activated charcoal particles was applied. Although the adsorption of carbon dioxide on activated charcoal has been employed in many researches [19,20], it was applied for the first time in a cocurrent downflow gas–solid circulating fluidized bed in this study.

In this work, experiments were carried out to measure the steady-state adsorption of CO_2 on the activated charcoal particles in the downer. Using this method, the characteristics of gas–solids mass transfer were investigated under different operating conditions.

2. Experimental method and apparatus

Experiments were carried out at atmospheric pressure and room temperature (20 °C). Air was used as the fluidizing gas, and CO_2 gas was the tracer. The solid phase (adsorbent) is GH-13 activated charcoal with an average diameter of 337 μm, a bulk density of 410 kg/m^3 and a skeleton density of 1270 kg/m^3.

Due to the adsorption, CO_2 tracer concentration decreases along the downer. By monitoring the change of trace concentration at different axial locations, the amount of CO_2 adsorption by the activated charcoal can be obtained. To ensure accuracy, the used charcoal was not re-circulated back to the downer top. Fresh charcoal particles were used for all adsorption tests.

A model for mass transfer was established with the following assumptions:

(1) In the downer, both the gas and solids flow downward in the same direction of gravity and the radial distributions of gas and solids velocities are uniform. Therefore, a

one-dimensional model can be used to describe the mass transfer in the downer.

(2) The mass transfer coefficient, gas diffusion coefficient and gas velocity all remain constant in the entire riser. Due to the low concentration of tracer gas, its adsorption has negligible effect on the gas flow rate.

(3) The axial gas dispersion is due to the turbulent movement and can be described by the dispersion coefficient, E_a.

Based on these assumptions, a mass balance across a height increment in the downer gives:

$$u_g\left(\frac{\partial c}{\partial x}\right) - E_a\left(\frac{\partial^2 c}{\partial x^2}\right) + G_s\left(\frac{\partial q}{\partial x}\right) + \varepsilon\left(\frac{\partial c}{\partial t}\right) + \rho_p(1-\varepsilon)\left(\frac{\partial q}{\partial t}\right) = 0 \quad (1)$$

For steady-state conditions, $\partial c/\partial t = 0$, Eq. (1) can be simplified to:

$$E_a\left(\frac{d^2 c}{dx^2}\right) - u_g\left(\frac{dc}{dx}\right) - G_s\left(\frac{dq}{dx}\right) = 0 \quad (2)$$

For the steady-state mass transfer, the kinetic equation for gas adsorption is:

$$\gamma = \gamma_a = \gamma_b = \rho_b\left(\frac{dq}{dt}\right) = K_F a(c - c^*) = k_f a(c - c_i) = k_s a\rho_p(q_i - q) \quad (3)$$

here k_f and k_s are the mass transfer coefficients of the gas side and the solids side. k_s is related to D_e, the effective coefficient of diffusion in the solids phase, by the following equation [17];

$$\beta k_s a = \frac{15 D_e(1-\varepsilon)}{R^2} \quad (4)$$

Since $dt = dx/v_s$, one has

$$\frac{dq}{dx} = \frac{dq}{d(v_s t)} = \left(\frac{1}{v_s}\right)\left(\frac{dq}{dt}\right) \quad (5)$$

Combining Eqs. (3) and (5), one has:

$$\frac{dq}{dx} = \frac{K_F a(c - c^*)}{\rho_b v_s} \quad (6)$$

According to the adsorption equilibrium, the distribution of adsorption in the gas and the solids phases at the interface is

$$c^* = \frac{q}{\beta} \quad (7)$$

Therefore, the basic gas–solids adsorption equations are given by Eqs. (2), (6) and (7).

In addition, the boundary conditions are:

$$x = 0, \quad c = c_0 \quad (8)$$

$$x = 0, \quad q = 0 \quad (9)$$

$$x = L, \quad \frac{dc}{dx} = 0 \quad (10)$$

A mass balance for the tracer gas from the top of the bed ($x = 0$) to the location x gives:

$$q = \frac{u_g(c_0 - c)}{G_s} \quad (11)$$

Substituting Eq. (11) into the equations for adsorption and making them dimensionless will yield the following expressions:

$$\frac{1}{Pe_1}\left(\frac{d^2 C}{d^2 Z}\right) - \frac{dC}{dZ} - (1+\Phi)\frac{C - (\Phi/(1+\Phi))}{Pe_2} = 0,$$

$$Z = 0, \quad C = 1; \quad Z = 1, \quad \frac{dc}{dZ} = 0 \quad (12)$$

where

$$C = \frac{c}{c_0}, \qquad Z = \frac{x}{L}, \qquad Pe_1 = L\frac{u_g}{E_a}, \qquad Pe_2 = \frac{u_g}{K_F a L}, \qquad \Phi = \frac{u_g}{G_s \beta}$$

Solving the above equation provides the following analytic solution for the dimensionless concentration of the CO_2 tracer gas along the downer:

$$C = \frac{\eta e^{(\eta+\xi z)} - \xi e^{(\xi+\eta z)} + \Phi(\eta e^{\eta} - \xi e^{\xi})}{(1+\Phi)(\eta e^{\eta} - \xi e^{\xi})} \quad (13)$$

where

$$\xi = \frac{Pe_1}{2}\left\{1 + \left[1 + \frac{4(1+\Phi)}{Pe_1 Pe_2}\right]^{1/2}\right\} \quad (14)$$

$$\eta = \frac{Pe_1}{2}\left\{1 - \left[1 + \frac{4(1+\Phi)}{Pe_1 Pe_2}\right]^{1/2}\right\} \quad (15)$$

Eqs. (13)–(15) were used to analyze the experimental data.

The experimental apparatus is shown in Fig. 1. The total height of the apparatus was about 5 m. The inner diameter of the Plexiglas downer was 33 mm and its height was 2.81 m. There were six sampling taps, located at 0.0, 0.58, 1.16, 1.73, 2.26 and 2.81 m below the downer entrance. Mixed with dry air, the tracer CO_2 entered the reactor via a single nozzle located at the downer center as air distributor (5). The activated charcoal particles were fed through a valve (4-E) and then flow into Venture tube (6), where the gas mixture was mixed and contacted with the adsorbent particles. Mass transfer took place between gas and solids as they flow downwards in the downer. At the bottom of the reactor, gas and solids were separated rapidly by a uniflow cyclone (10). The solid particles then flow into the lower container (12). In order to stabilize the gas pressure and to ensure stable operation of the uniflow-cyclone, solid particles were first transported into the bottom container (14) where they were lifted to the upper container (2) by dry and CO_2 free air. Valves D and C were used to measure the solids circulation rate and to remove the used adsorbent particles. Tank (11) was used as supply storage when starting to run the system, from which fresh charcoal particles were lifted by CO_2 free air to the upper container (2). Valve C was open when the system was started

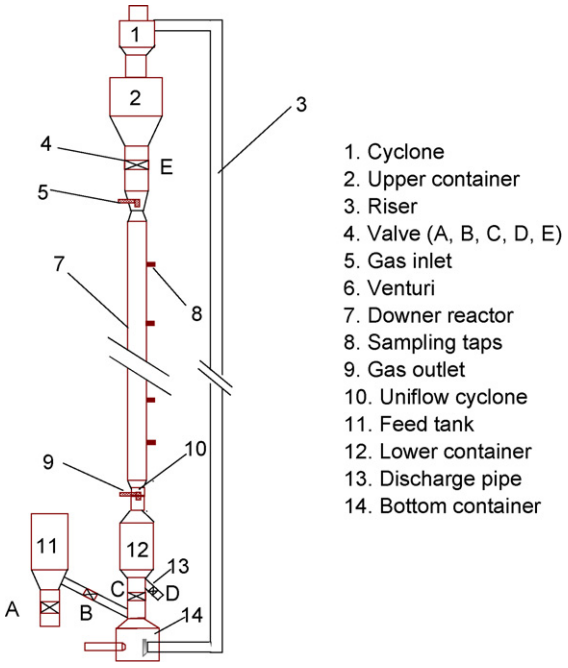

Fig. 1. Schematic diagram of the downer apparatus.

to achieve steady solids flow conditions, but were closed when CO_2 tracer was introduced to start the adsorption experiments.

The tracer gas was sampled simultaneously from the six taps along the downer. Each tap was covered by a fine mesh to prevent the particles from entering into the sampling line. The carbon dust on the fine mesh may adsorb the tracer gas, however the amount of dust is too small and so is the adsorbed CO_2 to affect the measurement. The dust formed on the fine mesh will soon reach equilibrium and practically incapable of affecting the concentration of CO_2 in the sampled gas. The concentration of CO_2 in each gas sample was then determined by chromatography, to give the axial distribution of CO_2 concentration in the downer. With the experimentally measured axial distribution profile of tracer CO_2 concentration (c_i/c_0), the model parameters Pe_1 and Pe_2 and the corresponding E_a and K_F were evaluated with the Marquardt non-linear regression method according to Eqs. (13)–(15). Marquardt non-linear regression is an efficient iterative method which is a combination of Linear Descent (works well for early iterations) and Gauss–Newton method (works well for later iterations) to find the best fit values for experimental data.

3. Results and discussion

3.1. Axial distribution profile of the CO_2 concentration

Fig. 2 shows the axial distributions of CO_2 concentration measured under different operating conditions. It is found that the concentration of CO_2 decreases as the gas and solids flow downward because of gas–solids mass transfer. The concentration of CO_2 decreases more dramatically upon initial gas and solids contact and then more gradually down the bed. Since the extent of the decrease is governed by the gas–solids mass transfer rate, the above results show that the initial gas and solids mass transfer is very high and that the adsorption between the gas and solids become gradually saturated below.

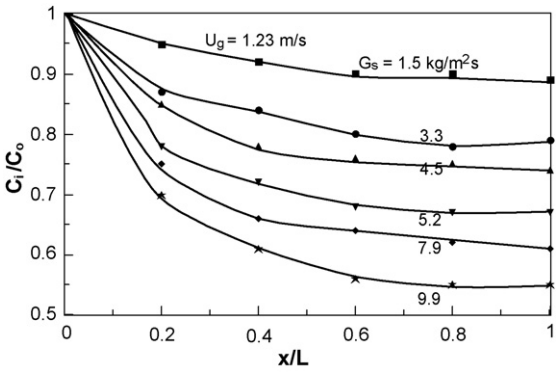

Fig. 2. Axial distribution profiles of the tracer CO_2 concentration.

Further down, the rate of mass transfer approaches zero and there is no further visible change in the concentration of CO_2 along the axial direction. This also means that adsorption has reached equilibrium.

3.2. Axial dispersion coefficient E_a

The value of axial dispersion coefficient evaluated from the experimental data ranges from 0.25 to 0.6, which is an order of magnitude lower than that in the riser [18]. This is due to the uniform gas and solids flow in the direction of gravity. With reduced axial gas and solids dispersions, the reaction selectivity in the downer is much better than that in the riser.

The operating conditions such as solids circulation rate, G_s, and superficial gas velocity, u_g, have very significant effect on the axial gas dispersion coefficient, E_a. It is obvious that the solids concentration always increase with the solids circulation rate [5]. The gas flow turbulence increases with increasing solid concentration. However at high solid concentrations (well above the solid concentrations in this study) the eddies may be broken by the solid particles and consequently the flow may become less turbulent (Fig. 3a). Increasing gas velocity also enhances the turbulent movement in the gas–solids flow and consequently raises the axial gas dispersion coefficient (Fig. 3b).

In order to describe more clearly the effect of operating conditions on the axial gas dispersion coefficient, an empirical correlation based on non-dimensional numbers was obtained by linear regression:

$$Pe_1 = 0.226 Re_p^{0.449} m^{-0.302} \tag{17}$$

where Pe_1 is the axial dispersion Peclet number indicating the proximity to plug flow, $Re_p = (2F_gR)/\mu$ is the particulate Reynolds number (F_g is the mass flow rate of the gas) and m is a dimensionless group related to the relative solids/gas flow ratio:

$$m = \frac{G_s}{u_g \rho_p} = \frac{v_s(1-\varepsilon)}{u_g \varepsilon} \tag{18}$$

The relative error between the predictions by Eq. (17) and the experimental data is within 7%.

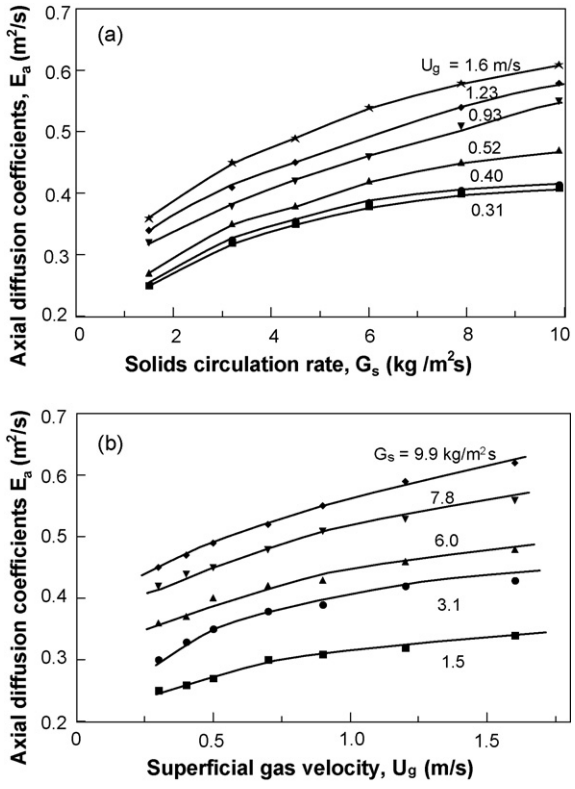

Fig. 3. The effect of operating conditions on the axial dispersion coefficient, E_a. (a) The effect of solids circulation rate and (b) the effect of superficial gas velocity.

3.3. The overall mass transfer coefficient

The effect of the solids circulation rate and gas velocity on the overall mass transfer coefficient is shown in Fig. 4. When the gas velocity is fixed, the changes of G_s have no significant effect on the overall mass transfer coefficient K_F. While the increase of solids concentration associated with increased G_s enhances turbulent mass transfer between gas and solids, it also increases the probability of particle cluster formation, which in turn decreases the gas–solids contact efficiency. It seems that those two effects cancel out each other so that the effect of the solids circulation rate on overall mass transfer coefficient appears to be negligible. Fig. 4 also shows that the overall mass transfer coefficient K_F

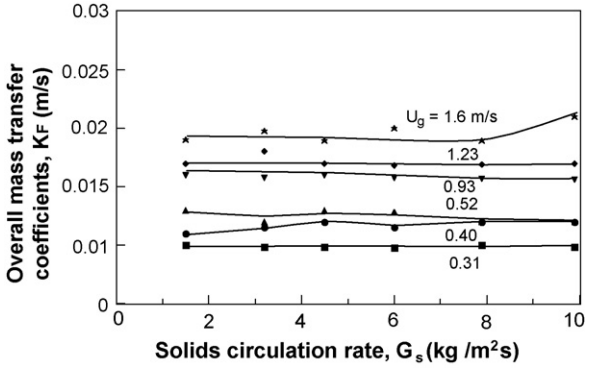

Fig. 4. The effect of G_s and u_g on the overall mass transfer coefficient, K_F.

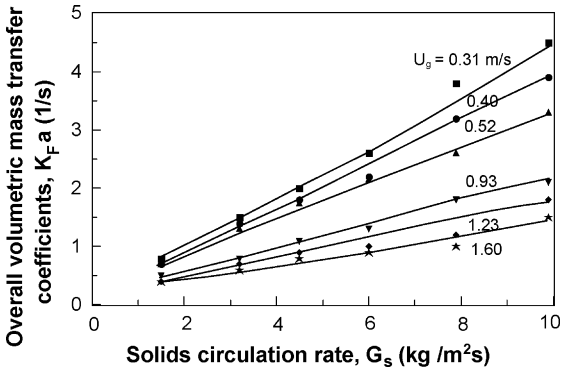

Fig. 5. The effects of G_s and u_g on the overall volumetric mass transfer coefficient, K_Fa.

increases considerably with the gas velocity while G_s are kept constant. This is because higher gas velocity induces more turbulence in the gas flow, and therefore reduces the resistance to mass transfer in the gas film and enhance the gas–solids mass transfer rate.

The effect of operating conditions on the overall volumetric mass transfer coefficient, K_Fa, is presented in Fig. 5. With increasing solids circulating rate, the specific surface area of the solids, a, is increased so that the overall volumetric mass transfer coefficient is higher. On the other hand, the increase of gas velocity results in an increase of the bed voidage and a decrease of the specific surface area, so that K_Fa, the quantity of mass transfer per unit volumetric bed, is decreased with gas velocity even though the mass transfer coefficient per unit surface area (Fig. 4) is increased.

An empirical correlation for the overall volumetric mass transfer coefficient with the operating conditions was also obtained:

$$Pe_2 = \frac{u_g}{K_F a L} = 0.000185 Re^{0.618} m^{-0.983} \quad (19)$$

with a maximum relative error of 9%.

3.4. Mass transfer coefficient at the solids side

From Eq. (4), the mass transfer coefficient from the solids side, k_s, is found to be independent of G_s and u_g. However, because of the effects of solids circulation rate and superficial gas velocity on the specific surface area of the solids, the volumetric mass transfer coefficient, k_sa, increases with the increase of solids circulation rate and decreases with the increase of gas velocity (Fig. 6).

3.5. Mass transfer coefficient at the gas side

Fig. 7 shows that the variation of the mass transfer coefficient for gas sides with G_s are not very significant. It also shows that k_f increases significantly as u_g increases when G_s are kept constant. Because the mass transfer coefficient on the solids side is independent of the operating conditions, the variation trend for k_f follows that for K_F.

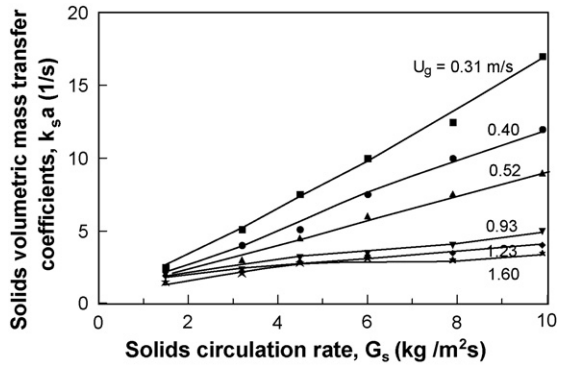

Fig. 6. The effects of G_s and u_g on the solid phase volumetric mass transfer coefficient, $k_s a$.

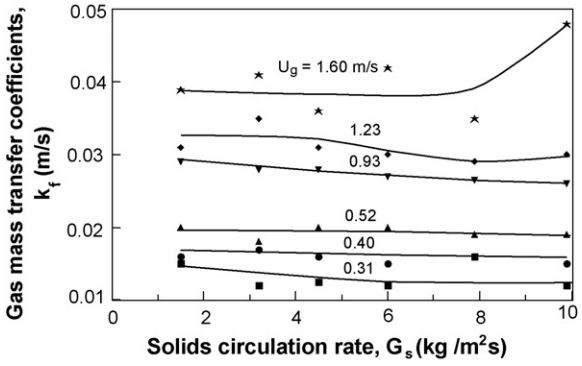

Fig. 7. The effects of operating conditions on the gas phase mass transfer coefficient, k_f.

The increase of solids concentration results in the increase of the specific surface area in the bed, so the gas volumetric mass transfer coefficient, $k_f a$, become higher (Fig. 8). As u_g increases, k_f is also increased but the specific surface area is decreased. As a result, $k_f a$ demonstrates a general tendency to decrease with u_g (Fig. 8). This also indicates that the gas velocity has more influence on the surface area than on the mass transfer at the gas side.

3.6. Overall considerations

In summary, the increase of solids circulation rate increases the volumetric mass transfer coefficient and consequently increases the mass transfer quantity between gas and solids, even though the variation of G_s has only a little influence on k_f and K_F. However, if the increase of the solids circulation rate goes beyond the range of the present experimental conditions, the magnitude of the gas–solids mass transfer coefficient may drop because of the increased probability of particle clustering with increasing G_s. Similarly, the increase of u_g can improve the gas–solids mass transfer, but it also leads to the decrease of the volumetric mass transfer coefficient, so that the overall mass transfer coefficient would be decreased. For these reasons, the optimum operating conditions of G_s and u_g must be selected carefully when designing a reactor, to optimize the gas–solids mass transfer.

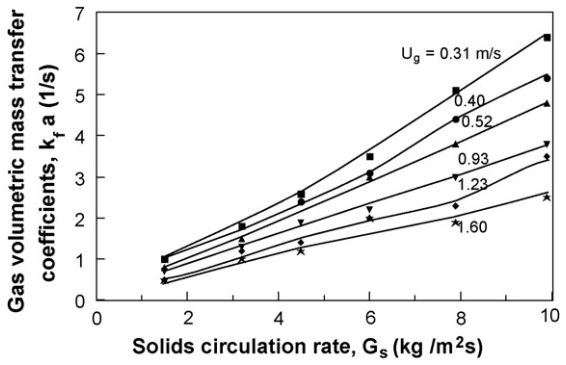

Fig. 8. The effect of operating conditions on the gas volumetric mass transfer coefficient, $k_f a$.

4. Conclusion

The method of steady-state adsorption was adopted to study the characteristics of gas–solids mass transfer and the axial distribution profiles of the tracer CO_2 concentration in the downer. Based on a one-dimensional flow model and the adsorption kinetics, mass transfer coefficient and axial dispersion coefficients were obtained by means of a non-linear regression method (the Marquardt method).

It is found that the solids circulation rate and superficial gas velocity have no effect on the mass transfer at the solids side, but have various effects on the mass transfer coefficient at the gas side and consequently on the overall mass transfer coefficient. In comparison with G_s, u_g has greater influence on k_f and K_F. Thus, a higher gas velocity can enhance the gas–solids mass transfer.Based on the experimental results, two empirical correlations for the axial dispersion coefficient and the overall mass transfer coefficient were obtained:

$$Pe_1 = \frac{Lu_g}{E_a} = 0.226 Re^{0.499} m^{0.302}$$

$$Pe_2 = \frac{u_g}{K_F a L} = 0.000185 Re^{0.618} m^{-0.983}$$

with $m = G_s/(u_g \rho_p) = v_s(1-\varepsilon)/(u_g \varepsilon)$.

They fit the experimental data very well with relative errors below 7% and 9%, respectively. More experimental data are required to quantify the mass transfer process in downer in a wide range of variables. The obtained correlations in this study should be carefully applied for scale-up purposes.

References

[1] B. Gross, M.P. Ramage, FCC reactor with a downflow reactor riser, U.S. Patent 4,385,985 (1983).
[2] B. Gross, Heat balance in FCC process and apparatus with downflow reactor riser. U.S. Patent 4,411,773 (1983).
[3] P.K. Niccum, D.P. Bunn, Catalytic cracking system, U.S Patent 4,514,285 (1985).
[4] F. Wei, Y. Jin, Z.-Q. Yu, N.-J. Gan, Z.-W. Wang, Application of phosphor tracer technique to the measurement of solids RTD in circulating fluidized bed, J. Chem. Ind. Eng. China (Chinese Edition) 2 (1994) 230–235.
[5] J.-X. Zhu, Z.-Q. Yu, Y. Jin, J.R. Grace, A. Issangya, Cocurrent downflow circulating fluidized bed (downer) reactors—a state of the art review, Can. J. Chem. Eng. 73 (1995) 662–677.

[6] J.-X. Zhu, F. Wei, Recent developments of downer reactors and other types of short contact reactors, in: J.F. Large, C. Laguerie (Eds.), Fluidization VIII, Engineering Foundation, New York, 1996, pp. 501–510.
[7] E. Aubert, D. Barreteau, T. Gauthier, R. Pontier, Pressure profiles and slip velocities in a co-current downflow fluidized bed reactor, in: A.A. Avidan (Ed.), Circulating Fluidized Bed Technology IV, AIChE, New York, 1994, pp. 389–420.
[8] P.M. Herbert, T.A. Gauthier, C.L. Briens, M.A. Bergougnou, Flow study of a 0.05 m diameter downflow circulating fluidized bed, Powder Technol. 96 (1998) 255–261.
[9] H. Zhang, J.-X. Zhu, M.A. Bergougnou, Hydrodynamics in downflow fluidized beds (1): solids concentration profiles and pressure gradient distributions, Chem. Eng. Sci. 54 (22) (1999) 5461–5470.
[10] H. Zhang, J.-X. Zhu, M.A. Bergougnou, Flow development in a gas–solids downer fluidized bed, Can. J. Chem. Eng. 77 (1999) 194–198.
[11] J.-X. Zhu, Y. Ma, H. Zhang, Gas–solids contact efficiency in the entrance region of a co-current downflow fluidized bed (downer), Trans. I. Chem. 77 (1999) 151–158.
[12] J.F. Richardson, A.G. Backhtier, Inst. Chem. Eng. 36 (1958) 283–287.
[13] J. Szckely, Symposium on interaction between fluid and particles, Inst. Chem. Eng. 6 (1962) 197.
[14] J.M. Coulson, J.F. Richardson, Chemical Engineering, vol. 3, Pergamon Press, 1971, pp. 504–533.
[15] G.J. Gregg, K.S.W. Sing, Adsorption. Surface Area and Porosity, Academic Press, 1967.
[16] J. Andrieu, J.M. Smith, Gas–liquid reaction in chromatographic columns, Chem. Eng. J. 20 (1980) 211–218.
[17] C.H. Jury, An improved version of the rate equation for molecular diffusion in a dispersed phase, AIChE J. 13 (1967) 1124–1126.
[18] G.-H. Luo, G.-L. Yang, Axial gas dispersion in fast fluidized beds, in: Proceedings of the 5th Chinese National Conference on Fluidization, Beijing, China, May, 1990, pp. 155–158.
[19] N.D. Del Vecchio, S. Barghi, S. Primak, J.E. Puskas, New method for monitoring adsorption column saturation and regeneration II, Chem. Eng. Sci. 59 (2004) 2389–2400.
[20] A. Min, A.T. Harris, Influence of carbon dioxide partial pressure and fluidization velocity on activated carbons prepared from scrap car tyre in a fluidized bed, Chem. Eng. Sci. 61 (2006) 8050–8059.